



A sandwich mixed (phthalocyaninato) (porphyrinato) europium triple-decker: Balanced-mobility, ambipolar organic thin-film transistor



Xia Zhang, Yanli Chen*

Shandong Provincial Key Laboratory of Fluorine Chemistry and Chemical Materials, School of Chemistry and Chemical Engineering, University of Jinan, Jinan 250022, China

ARTICLE INFO

Article history:

Received 10 October 2013

Accepted 25 October 2013

Available online 5 November 2013

Keywords:

Phthalocyanine
Porphyrin
Triple-decker
Ambipolar
OTFT

ABSTRACT

A new sandwich mixed (phthalocyaninato) (porphyrinato) europium triple-decker (TPP)Eu₂[Pc(OPh)₈]₂ (**1**), [TPP = dianion of 5,10,15,20-tetrakisporphyrin; Pc(OPh)₈ = dianion of 2,3,9,10,16,17,23,24-octa(phenoxy)phthalocyanine], has been synthesized and characterized by a series of spectroscopic methods including MALDI-TOF mass spectrometry, ¹H NMR spectroscopy, electronic absorption and infrared spectroscopy. The electrochemical property of **1** has been studied by cyclic voltammetry. Constructing the target triple-decker by coordination bonding between an europium ion and isoindole/tetrapyrrole nitrogen atoms from *n*-type double-decker (Eu[Pc(OPh)₈]₂) and *p*-type porphyrin (H₂TPP) units, not only ensures the good solubility in conventional organic solvents, but more importantly successfully tunes the HOMO and LUMO levels into the range of ambipolar organic semiconductors required on the basis of electrochemical studies over **1**. Using a solution-based quasi-Langmuir–Shäfer (QLS) method, the thin solid films of **1** were fabricated. The structure and properties of the thin films were investigated by UV–vis absorption spectra, X-ray diffraction (XRD) and scanning electron microscopy (SEM). Experimental results indicated the film crystallinity and general molecular order for (TPP)Eu₂[Pc(OPh)₈]₂ molecules in the QLS films. Organic thin-film transistor (OTFT) fabricated from the QLS films of **1** was revealed to show ambipolar properties that have never been revealed for devices fabricated from a single-phthalocyanine/porphyrin mixed component using solution processable technique, with the highly balanced mobilities for holes and electrons of 0.04 cm² V⁻¹ s⁻¹ and 0.08 cm² V⁻¹ s⁻¹, respectively.

© 2013 Elsevier B.V. All rights reserved.

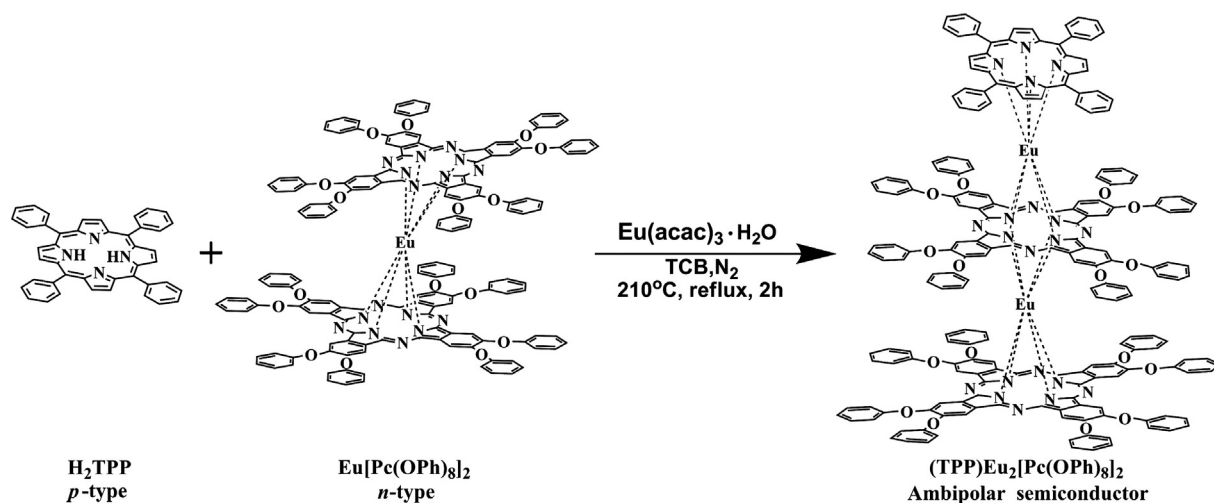
Research on organic semiconductors for thin-film transistors (OTFTs) has made great progress since the first report on *p*-type OTFTs in 1986 [1]. Ambipolar OTFTs allowing dual operation of both *p* and *n* types are highly desired for practical application in integrated circuits like high gain complementary metal-oxide-semiconductor inverters and light emitting devices [2–6]. In particular, ambipolar OTFT devices with highly balanced carrier mobility for both holes and electrons, and solution-processability that ensure low-cost fabrication have therefore attracted great research interests in the past decade [7–9]. Despite great efforts paid in this direction, OTFTs meeting the above-mentioned requirements still remain rare. Effective methods thus far developed for fabricating ambipolar OTFTs include blending two organic components [10,11] and modifying gate insulator or electrodes [12–14]. The first ambipolar behavior was obtained for the OFETs as early as 1990 with the sandwich-type bis(phthalocyaninato) rare earth double-decker complexes (MPc₂, M = Tm, Lu), which exhibited a *p*-type behavior in air and a *n*-type behavior under vacuum [15]. However, the most attractive approach appears to be the utilization of single-component organic semiconductor with suitable energy for both HOMO and LUMO, balanced carrier mobility for both holes and electrons, and solution processability. To our knowledge, the best achievement of solution-

processed ambipolar OTFT devices fabricated using single-component phthalocyanine-based molecular material was reported by Jiang and co-workers, with (*p*-fluoro)phenoxy-substituted tris(phthalocyaninato) europium complex as semiconductor, displaying carrier mobility of 0.24 and 0.042 cm² V⁻¹ s⁻¹ for holes and electrons, respectively [16].

The pioneering work by Checcoli and co-workers reported 5,10,15,20-tetraphenylporphyrin as a *p*-type organic semiconductor with a hole mobility as high as 0.007 cm² V⁻¹ s⁻¹ [17]. Recently, the solution-based OTFTs for a sandwich-type bis(phthalocyaninato) europium complex Eu[Pc(OPh)₈]₂ have been revealed to show good *n*-type device characteristics with the electron mobility of 0.54 cm² V⁻¹ s⁻¹ in our preliminary studies [18]. With this background in mind, we focus our attention on exploring high-performance ambipolar semiconducting materials with a balanced charge-carrier mobility for both hole and electron through suitable molecular design as well as efficient self-assembly process. In this communication, a new sandwich mixed (phthalocyaninato) (porphyrinato) europium triple-decker (TPP)Eu₂[Pc(OPh)₈]₂ (**1**), [TPP = dianion of 5,10,15,20-tetrakisporphyrin; Pc(OPh)₈ = dianion of 2,3,9,10,16,17,23,24-octa(phenoxy)phthalocyanine], was synthesized (Scheme 1). The material design strategy in this study grows out of previous research using *n*-type double-decker (Eu[Pc(OPh)₈]₂) and *p*-type 5,10,15,20-tetraphenylporphyrin (H₂TPP) as the building blocks for constructing a new semiconductor [17,18]. The OTFT devices have been prepared from triple-decker **1** by means

* Corresponding author.

E-mail address: chm_chenyl@ujn.edu.cn (Y. Chen).



Scheme 1. Synthesis of the sandwich mixed (phthalocyaninato) (porphyrinato) europium $(\text{TPP})\text{Eu}_2[\text{Pc}(\text{OPh})_8]_2$ (**1**).

of solution-based *quasi-Langmuir-Shäfer* (QLS) method [19] and the balanced mobilities for both electrons and holes have been determined in the present work.

The mixed (phthalocyaninato) (porphyrinato) europium complex $(\text{TPP})\text{Eu}_2[\text{Pc}(\text{OPh})_8]_2$ was prepared according to the published procedures [20–23]. A mixture of $\text{Eu}[\text{Pc}(\text{OPh})_8]_2$, metal free porphyrin H_2TPP and $\text{Eu}(\text{acac})_3 \cdot n\text{H}_2\text{O}$ in the presence of TCB was heated to reflux for 2 h under a slow stream of nitrogen (Scheme 1). Repeated chromatography followed by recrystallization from CHCl_3 and CH_3OH gave pure compound as a black green powder in good yield of 42.5%. UV–vis [CH_2Cl_2 ; λ_{max} , nm ($\log(\epsilon)$, $\text{M}^{-1} \text{cm}^{-1}$): 360(6.16), 412(6.03), 628(5.72) 720(5.45)]; ^1H NMR (400 MHz, CDCl_3): δ 12.943 (s, 4H, Por-Ph- H_{α}^{endo}), 12.289 (s, 8H, Pc- H_{α}), 9.697 (s, 8H, Pc- H_{α}), 8.945–8.965 (d, 16H, Pc-Ph- H_{α}), 8.836–8.854 (d, 4H, Por-Ph- H_{α}^{endo}), 8.355–8.394 (t, 16H, Pc-Ph- H_m), 8.204–8.244 (t, 4H, Por-Ph- H_p), 8.088–8.127 (t, 8H, Pc-Ph- H_p), 7.887–7.907 (d, 16H, Pc- H_{α}), 7.796–7.835 (t, 16H, Pc- H_m), 7.511–7.548 (t, 8H, Pc- H_p), 6.961–6.996 (t, 4H, Por-Ph- H_{α}^{exo}), 5.209–5.224 (t, 4H, Por-Ph- H_m^{exo}), 3.406 (s, 8H, Por- H_{β}). MALDI-TOF MS: an isotopic cluster peaking at m/z 3417.63, Calcd for $\text{C}_{204}\text{H}_{123}\text{Eu}_2\text{N}_{20}\text{O}_{16}$, $[\text{M}]^+$, 3416.83; Main IR (KBr) ν_{max} (cm^{-1}): 2922, 2785, 2704 (alkyl C–H stretching), 1587 (benzene stretching), 1485 (pyrrole stretching), 1448 (isoindole stretching), 1398 (isoindole stretching), 1325 (pyrrole stretching), 1072 (coupling of isoindole deformation and aza stretching), 1020 (pyrrole-N in-plane bending), 883, 750 (Ar–H out-of-plane bending), 686 (benzene C–H stretching). In addition, the target complex **1** exhibited good solubility in common organic solvents, making it possible to fabricate it into devices by solution processing.

Cyclic voltammetrical (CV) measurement of $(\text{TPP})\text{Eu}_2[\text{Pc}(\text{OPh})_8]_2$ in CH_2Cl_2 with four reversible one-electron oxidation couples and a couple of one-electron reductions observed the first oxidation and first reduction potential at +0.605 and –0.589 V (vs SCE), as shown in Fig. 1. Both the HOMO and LUMO energies at –5.05 and –3.86 eV thus derived for this compound just locate in the HOMO and LUMO energy range that are necessary for good *p*- and *n*-type organic semiconductors [24], respectively, ensuring the facilitation of both the hole and electron injections from the Au electrodes (with the work function of –5.1 eV). This actually reveals the potential of this triple-decker complex in ambipolar OTFT devices.

Ordered multilayers of $(\text{TPP})\text{Eu}_2[\text{Pc}(\text{OPh})_8]_2$ were prepared by the QLS method. The QLS layers were then deposited onto hexamethyldisilazane (HMDS)-treated SiO_2/Si substrates. The quality of the QLS films, it is in fact the information concerning the molecular ordering in the film, could be assessed using X-ray diffraction technique. As shown in Fig. 2, the out-of-plane (OOP) XRD diagram of QLS films of **1** deposited on SiO_2/Si substrate shows a well-defined low-angle

diffraction peak at $2\theta = 4.18^\circ$, which is ascribed to the diffractions from the (001) plane, indicating the long-range molecular ordering across the thickness of the QLS films [18,25]. The OOP d-spacing calculated according to the Bragg equation is about 2.11 nm, which corresponds to a periodic distance between two adjacent triple-decker molecules of **1** along the direction of the substrate surface normal. Judging from the diagonal dimension of the $(\text{TPP})\text{Eu}_2[\text{Pc}(\text{OPh})_8]_2$ molecule, 2.20 nm, on the basis of single crystal X-ray diffraction results [16,26–28], the orientation angle between the phthalocyanine ring in the triple-decker molecule and substrate surface of ca. 73.5° is deduced. Consequently, the triple-decker molecules of **1** are oriented nearly perpendicular to the substrate surface in *H*-aggregation mode (inset of Fig. 2) [29]. A higher-order diffraction is found at 0.37 nm for the films of triple-decker **1**, which can be attributed to the formation of efficient π – π stacking with face-on orientations [28]. It is therefore expected that $(\text{TPP})\text{Eu}_2[\text{Pc}(\text{OPh})_8]_2$ films would be able to adopt 3-D conduction channels that would decrease the barrier of charge transport over that of the QLS films [30], and in turn contribute to the excellent hole and electron mobility revealed for the devices fabricated with **1** (*vide infra*). Intermolecular interactions between adjacent molecules in the QLS films were characterized by UV–vis spectroscopy. As shown in Fig. 3, $(\text{TPP})\text{Eu}_2[\text{Pc}(\text{OPh})_8]_2$ in CH_2Cl_2 solution displays intense Q bands at 628 and 720 nm and the Soret bands at 360 and 412 nm, which are analogous to those reported for mixed (phthalocyaninato) (porphyrinato) rare earth complexes [31,32]. However, after being fabricated into the QLS films, the main Q bands were broadened and

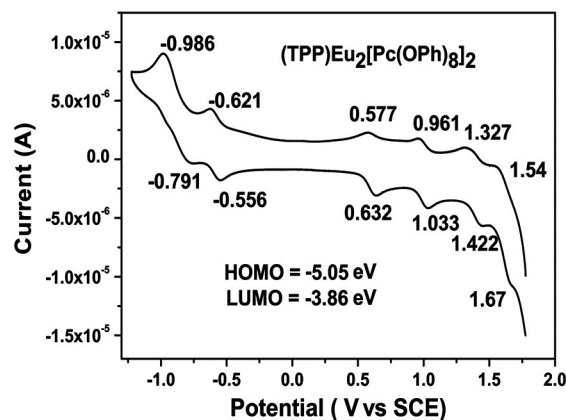


Fig. 1. Cyclic voltammogram (CV) of $(\text{TPP})\text{Eu}_2[\text{Pc}(\text{OPh})_8]_2$ in CH_2Cl_2 containing 0.1 mol L^{-1} $[\text{Bu}_4\text{N}][\text{ClO}_4]$ at a scan rate of 20 mV.

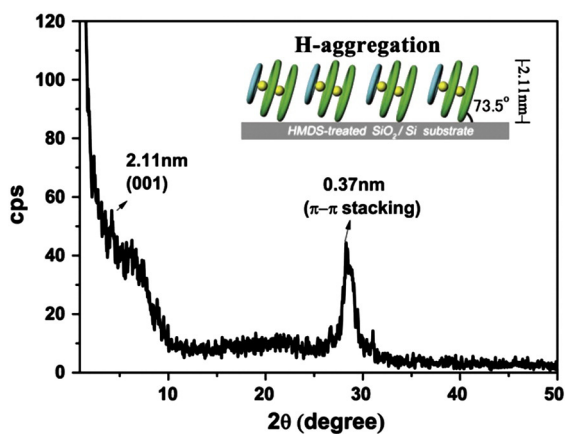


Fig. 2. X-ray diffraction pattern of the QLS films of compound **1** on SiO₂/Si substrate.

blue-shifted to 625 nm and 709 nm, respectively, while the Soret band at 412 nm was red-shifted to 420 nm, the point-dipole model of Kasha provides a rationale for the observed band shifts. The extreme cases are represented by a head-to-tail arrangement of the dipoles, which results in a red-shifted absorption band (*J*-aggregate), and a parallel arrangement of the dipoles (*H*-aggregate) with a blue-shifted absorption band. The red and blue shifted band components observed in the present case for the QLS films of triple-decker **1** represent an intermediate case with typical *H*- and *J*-aggregate [33]. That is, the triple-decker molecules take a “face-to-face” conformation and “edge-on” orientation in the QLS films, which is in line with the XRD result. SEM provides more information on the aspect of the QLS films of **1** and therefore allows us to correlate the morphology and electrical properties. Fig. 4 displays the morphology of the QLS films for triple-deckers **1** deposited on the HMDS-treated SiO₂/Si substrate. The surface of the QLS films of **1** presents a sheet-like morphology of ca. 600–800 nm in length with an evidence of crystalline feature, which is expected to cause fewer traps and/or defects localized around grain boundaries, and thus improving the carrier mobility [34].

OTFT devices were fabricated from (TPP)Eu₂[Pc(OPh)₈]₂ with a top-contact device configuration on hexamethyldisilazane (HMDS)-modified SiO₂ (300 nm)/Si substrates using the QLS technique [19]. Gold (Au) was used as drain and source electrodes. OTFT properties were evaluated under positive and negative bias in air/N₂ to explore the majority charge carrier type and device performance. Experimental data were analyzed using standard field-effect transistor equations [35]: $I_{ds} = (W/2L)\mu C_0(V_g - V_{th})^2$, where I_{ds} is the source–drain current, V_g is the gate voltage, C_0 is the capacitance per unit area of the dielectric

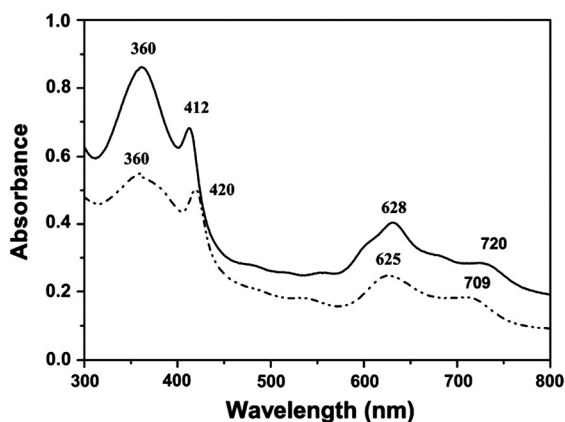


Fig. 3. UV-vis absorption spectra of compound **1** in dilute dichloromethane solution (5×10^{-7} mol L⁻¹, solid line) and QLS films (dash line).

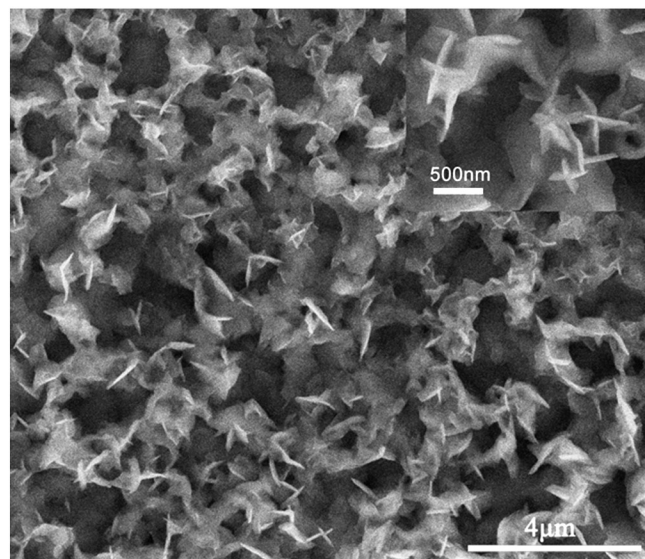


Fig. 4. SEM images of the QLS films of complex **1** deposited on HMDS-treated SiO₂/Si substrate (the inset is a magnified image).

layer, V_{th} is the threshold voltage, W and L are the channel width and length, respectively, and μ is the mobility in the saturation region. The mobility (μ) can then be calculated from the slope of the linear part of the V_g vs. $(I_{ds})^{1/2}$ plot (at $V_{ds} = -20$ or $+20$ V), respectively. The QLS films of (TPP)Eu₂[Pc(OPh)₈]₂ (**1**) exhibit both *p*-type and *n*-type characteristics with the carrier mobility up to 0.04 cm² V⁻¹ s⁻¹ for holes in air and 0.08 cm² V⁻¹ s⁻¹ for electrons in N₂, and the on/off ratio of $\sim 10^5$, as shown in Fig. 5. This seems to exhibit the best balanced-mobility for both electron and hole in terms of the ambipolar performance among the solution-processed phthalocyanine-based semiconductors reported thus far, suggesting the great potential of sandwich-type mixed (phthalocyaninato) (porphyrinato) rare earth complexes for applications in low-cost ambipolar organic electronics. It is worth noting that we did not observe *n*-channel transistor behavior of **1** in air, perhaps due to relative high LUMO energy of **1**, that still does not meet the requirement for an air-stable *n*-type OTFTs, which demands the value of LUMO energy lower than -4.0 eV to against the air-derived electron traps [36,37]. The design and synthesis of air-stable ambipolar semiconducting materials based on new sandwich-type tetrapyrrolo rare earth complexes with higher balanced-mobility are being developed in our lab.

In conclusion, we demonstrate a strategy for designing high-performance, solution-processable ambipolar, phthalocyanine-based OTFT materials with balanced-mobility for both hole and electron, which is based on constructing a triple-decker complex composing of both the good *n*-type bisphthalocyanines and the *p*-type porphyrin units. The suitable HOMO and LUMO energy levels associated with an intense intermolecular π – π stacking interaction in the film and highly organized film microstructures ensure the single-phthalocyanine/porphyrin mixed complex, (TPP)Eu₂[Pc(OPh)₈]₂, with the high and balanced mobilities for holes and electrons of 0.04 cm² V⁻¹ s⁻¹ and 0.08 cm² V⁻¹ s⁻¹, respectively. Such highly balanced-mobility values encourage chemists to design and prepare new molecules with optimized electronic structure and molecular packing for further improvements of OTFT devices.

Acknowledgment

Financial support from the Natural Science Foundation of China (21371073), Natural Science Foundation of Shandong Province (ZR2011BZ005) and University of Jinan in China is gratefully acknowledged.

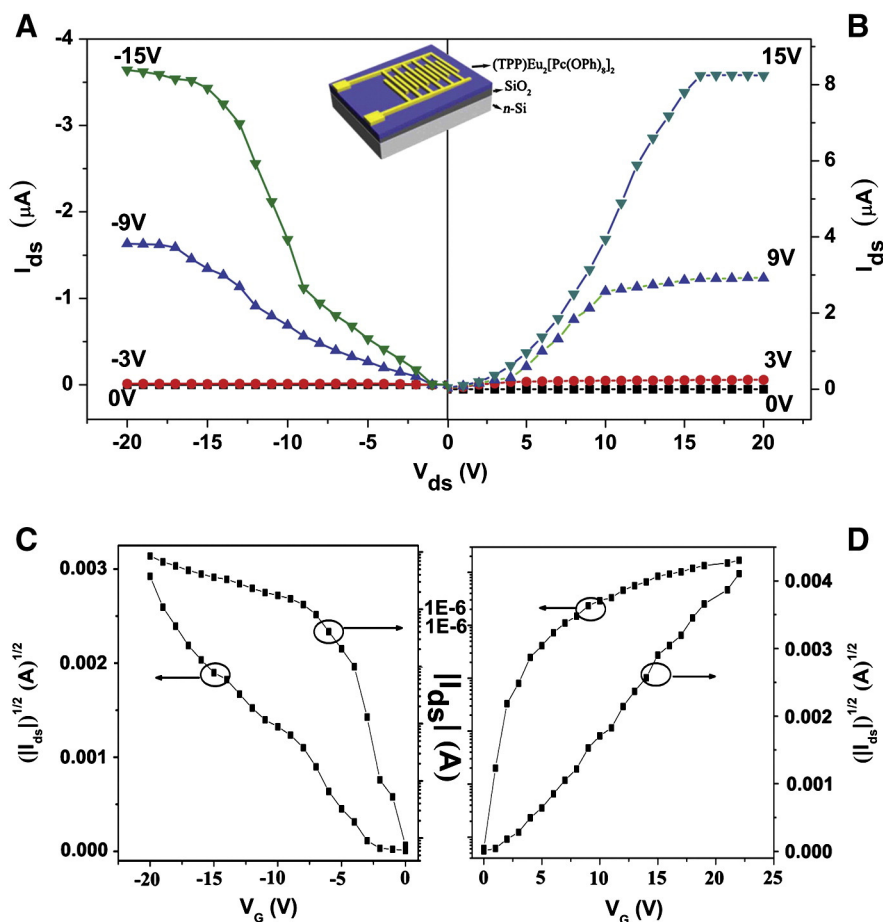


Fig. 5. Output characteristics (I_{ds} vs. V_{ds}) and transfer characteristics ($|I_{ds}|^{1/2}$ vs. V_g) of ambipolar OTFT device based on QLS films of **1** deposited on HMDS-treated SiO_2/Si (300 nm) substrate with Au top contacts obtained in air (A and C) and in N_2 (B and D). Current–voltage output plots (I_{ds} vs. V_{ds}) for p -channel (A) and n -channel (B) and the transfer characteristics of OTFTs at $V_{ds} = -20$ V for p -channel (C) and $V_{ds} = +20$ V for n -channel (D).

References

- [1] A. Tsumura, H. Koezuka, T. Ando, *Appl. Phys. Lett.* 49 (1986) 1210–1212.
- [2] L.L. Chua, J. Zaumseil, J.F. Chang, E.C.-W. Ou, P.K.-H. Ho, H. Sirringhaus, R.H. Friend, *Nature* 434 (2005) 194–199.
- [3] F.S. Kim, E. Ahmed, S. Subramanian, S.A. Jenekhe, *ACS Appl. Mater. Interfaces* 2 (2010) 2974–2977.
- [4] K. Walzer, B. Maennig, M. Pfeiffer, K. Leo, *Chem. Rev.* 107 (2007) 1233–1271.
- [5] M.A. Baldo, M.E. Thompson, S.R. Forrester, *Nature* 403 (2000) 750–753.
- [6] M.A. Baldo, D.F. O'Brien, Y. You, A. Shoustikov, S. Sibley, M.E. Thompson, S.R. Forrester, *Nature* 395 (1998) 151–154.
- [7] H. Usta, C. Risko, Z. Wang, H. Huang, M.K. Delimeroglu, A. Zhukhovitskiy, A. Facchetti, T.J. Marks, *J. Am. Chem. Soc.* 131 (2009) 5586–5608.
- [8] Y. Guo, G. Yu, Y. Liu, *Adv. Mater.* 22 (2010) 4427–4447.
- [9] P. Sonar, S.P. Singh, Y. Li, M. Soh, A. Dodabalapur, *Adv. Mater.* 22 (2010) 5409–5413.
- [10] R. Ye, M. Baba, K. Suzuki, K. Mori, *Jpn. J. Appl. Phys.* 46 (2007) 2878–2881.
- [11] R. Ye, M. Baba, K. Suzuki, K. Mori, *Solid State Electron.* 52 (2008) 60–62.
- [12] S. Noro, T. Takenobu, Y. Iwasa, H. Chang, S. Kitagawa, T. Akutagawa, T. Nakamura, *Adv. Mater.* 20 (2008) 3399–3403.
- [13] T. Yasuda, T. Tsutsui, *Chem. Phys. Lett.* 402 (2005) 395–398.
- [14] T. Yasuda, T. Tsutsui, *Jpn. J. Appl. Phys.* 45 (2006) 595–597.
- [15] G. Guillaud, M.A. Sadoun, M. Maitrot, J. Simon, M. Bouvet, *Chem. Phys. Lett.* 167 (1990) 503–506.
- [16] J. Kan, Y. Chen, D. Qi, Y. Liu, J. Jiang, *Adv. Mater.* 24 (2012) 1755–1758.
- [17] P. Checcoli, G. Conte, S. Salvasori, R. Paollesse, A. Bolognesi, A. Berliocchi, F. Brunetti, A. D'Amico, A. Di Carlo, P. Lugli, *Synth. Met.* 138 (2003) 261–266.
- [18] Y. Chen, D. Li, N. Yuan, J. Gao, R. Gu, G. Lu, M. Bouvet, *J. Mater. Chem.* 22 (2012) 22142–22149.
- [19] Y. Chen, M. Bouvet, T. Sizun, Y. Gao, C. Plassard, E. Lesniewska, J. Jiang, *Phys. Chem. Chem. Phys.* 12 (2010) 12851–12861.
- [20] D.K.P. Ng, J. Jiang, *Chem. Soc. Rev.* 26 (1997) 433–442.
- [21] J. Jiang, W. Liu, D.P. Arnold, *J. Porphyrins Phthalocyanines* 7 (2003) 459–473.
- [22] L.A. Lapkina, E. Niskanen, H. Rönkkömäki, V.E. Larchenko, K.I. Popov, A.Y. Tsvadze, *J. Porphyrins Phthalocyanines* 4 (2000) 588–590.
- [23] Y. Zhang, W. Jiang, J. Jiang, Q. Xue, *J. Porphyrins Phthalocyanines* 11 (2007) 100–108.
- [24] A.J. Bard, L.R. Faulkner, *J. Electroanal. Chem.* 199 (1984) 323–340.
- [25] T.J. Prosa, M.J. Winokur, J. Moulton, P. Smith, A.J. Heeger, *Macromolecules* 25 (1992) 4364–4372.
- [26] D. Li, H. Wang, J. Kan, W. Lu, Y. Chen, J. Jiang, *Org. Electron.* 14 (2013) 2582–2589.
- [27] J. Kan, H. Wang, W. Sun, W. Cao, J. Tao, J. Jiang, *Inorg. Chem.* 52 (2013) 8505–8510.
- [28] N. An, Y. Shi, J. Feng, D. Li, J. Gao, Y. Chen, X. Li, *Org. Electron.* 14 (2013) 1197–1203.
- [29] E.J. Meijer, D.M. de Leeuw, S. Setayesh, E. Van Veenendaal, B.-H. Huisman, P.W.M. Blom, J.C. Hummelen, U. Scherf, T.M. Klapwijk, *Nat. Mater.* 2 (2003) 678–682.
- [30] J. Lee, A.-R. Han, J. Kim, Y. Kim, J.H. Oh, C. Yang, *J. Am. Chem. Soc.* 134 (2012) 20713–20721.
- [31] G. Lu, Y. Chen, Y. Zhang, M. Bao, Y. Bian, X. Li, J. Jiang, *J. Am. Chem. Soc.* 130 (2008) 11623–11630.
- [32] J. Lu, D. Zhang, H. Wang, J. Jiang, X. Zhang, *Inorg. Chem. Commun.* 13 (2010) 1144–1147.
- [33] P. Ma, Y. Chen, N. Sheng, Y. Bian, J. Jiang, *Eur. J. Inorg. Chem.* 7 (2009) 954–960.
- [34] W. Wu, Y. Liu, Y. Wang, H. Xi, X. Gao, C. Di, G. Yu, W. Xu, D. Zhu, *Adv. Funct. Mater.* 18 (2008) 810–815.
- [35] S.M. Sze, *Physics of Semiconductor Devices*, John Wiley & Sons, New York, 1981, pp. 430–442.
- [36] B.A. Jones, A. Facchetti, M.R. Wasielewski, T.J. Marks, *J. Am. Chem. Soc.* 129 (2007) 15259–15278.
- [37] Z. Wang, C. Kim, A. Facchetti, T.J. Marks, *J. Am. Chem. Soc.* 129 (2007) 13362–13363.